Hindawi
Mobile Information Systems
Volume 2022, Article ID 5899657, 10 pages
https://doi.org/10.1155/2022/5899657

Research Article

Comparative Analysis of Strength Calculation for Railway's Flat Car Body Using Fuzzy Logic and Evolutionary Algorithms

Zhongliang Yang [1,2]

[1]*State Key Laboratory of Traction Power, Southwest Jiaotong University, Chengdu 610031, Sichuan, China*
[2]*Locomotive and Car Department, China State Railway Group Co. Ltd, Beijing 100844, China*

Correspondence should be addressed to Zhongliang Yang; yangzhongliang@my.swjtu.edu.cn

Received 28 April 2022; Revised 24 June 2022; Accepted 29 July 2022; Published 30 August 2022

Academic Editor: Mian Ahmad Jan

This article makes an in-depth analysis of different body strength calculation methods using fuzzy logic and evolutionary algorithm by taking the universal flat car body strength calculation as an example. For this study, a more scientific and reliable theoretical basis for the structural strength design and analysis of railway flat car surveying and mapping is considered. If the expansion and contraction of the jack are not synchronised while jacking the vehicle body with a jack when the vehicle is freshly manufactured and maintained, the vehicle body will be in a three-point support state. The 3-point support state will result in permanent deformation if a structure with low torsional stiffness is used. If the structure characterized by small torsional stiffness is adopted, the 3-point support state will produce permanent deformation. The safety factor specified in EN12663 is only 1.15, which shows that the Interim Provisions have the highest requirements for the design of vehicle body strength and the corresponding design cost. From the fatigue strength analysis, it can be seen that the difference between the maximum principal stress and the corresponding allowable stress at the node level with the maximum von Mises stress is high, which is not the dangerous position of the structure. The research shows that there are great differences in the provisions of jacking load in various specifications.

1. Introduction

As a representative of long-distance public transportation, railway transportation is particularly important [1]. At present, there are two main problems in the structural design of large-scale car body. First, under the condition of meeting the existing railway gauge, the bearing area of the car body is relatively limited due to the relatively general width of the car body and the relatively small length of the car body, which is often easy to occur, so that the volume of goods carried by the car body first seriously affects the bearing capacity of the car body of railway flat car [2]; secondly, because the total length of the car body is relatively limited, it can not meet the transportation requirements of large quantities and long goods. Therefore, it is particularly important to strengthen the strength design of railway flat car body [3, 4]. Taking the strength calculation of the general flat car body of a company as an example, this article compares different strength calculation methods and strength evaluation standards so as to deeply analyze the rationality of China's car body strength design code and provide a more scientific and reliable theoretical basis for the structural strength design and analysis of railway flat car surveying and mapping.

2. Literature Review

Mathematicians successively obtained the proof of convergence, error analysis model, and nonconforming convergence from mathematics, which made the finite element method have a solid mathematical theoretical foundation. Now, the finite element method has been widely recognized in the treatment of physics, mechanics, and engineering. During this period, a large number of general finite element programs have also been rapidly developed and widely used [5]. The finite element method is active in various

engineering fields. The reason is that it can solve various engineering problems. It has the characteristics of high calculation accuracy and flexible use. The general application of electronic computers is the material basis of its development.

From the 1970s to now, the finite element method has made many great breakthroughs, but the research focus has changed. It is mainly reflected in the expansion from static, linear, and deterministic analysis to dynamic, stability and material, geometric nonlinearity, and reliability analysis from solid mechanics to fluid, electromagnetic field, thermodynamics, geomechanics, biomechanics, and other problems [6].

The application of the finite element method in ship structure has revolutionized the resulting problem of traditional ship structure [7]. Among them, the most prominent aspect is that the traditional research of dividing the total transverse strength, total longitudinal strength, and local strength is changed into a seemingly unsolvable problem by the manual calculation method before the comprehensive analysis of the overall structure. The application of the finite element method can draw a conclusion conveniently and quickly.

That is gray areas. For example, there is no obvious boundary between tall and short, fat and thin. It can be said that it is a little, very, or very high, so the boundary (or critical condition) is fuzzy. Figure 1 shows the fuzzy logic system [8].

Fortran language is one of the earliest and most widely used computer languages. It is the abbreviation of formula translation. It was originally designed for numerical calculation. The first Fortran text was proposed in 1954 and was really used in 1956. Fortran is a process-oriented language. Process-oriented programming is mainly used to obtain results for large-scale engineering calculations or to complete a task. It has low requirements for the interface, and its advantage is its fast running speed [9].

The related software is called CAE software. CAE technology has a development history of more than 30 years. With the progress of graphics technology and database technology and the development of high-performance computer system, the research and application of CAE have also made rapid development, which has become the key means and the main design guarantee to realize the innovative design. CAE software has become a powerful assistant and effective tool for engineers to realize engineering innovation and product innovation. CAE technology has been paid more and more attention in China, and the automotive industry has generally realized the importance of CAE technology in improving product competitiveness [10]. In order to accelerate the development of new products and further improve the performance and scientific and technological content of products, CAE software can be used to analyze the structural strength and stiffness of existing models and the corresponding structural improvement so as to provide reference and verification methods for the research and development of new models.

To solve this research problem, Chawla, S. and others used a triangular element to wake up the contact stress analysis for the first time when analyzing the swept wing structure [11]. Zitrick and others derived the displacement method finite element model from the minimum potential energy principle, the force method from the minimum complementary energy principle, the hybrid method from the Hellinger–Reissner variational principle, the hybrid method finite element model from the modified complementary energy principle, etc. [12]. The research and analysis of Hoterova and others of the finite element method are active in various engineering fields. The reason is that it can solve various engineering problems and has the characteristics of high calculation accuracy and flexible use. The general application of electronic computers is the material basis for its development [13]. Xu and others believe that CAE is a comprehensive and knowledge-intensive discipline based on finite element analysis technology. The related software is called CAE software [14]. Wang and others worked out the calculation condition of static strength of high-speed car body based on EN12663 car body strength evaluation criteria and combined with the calculation characteristics of car body strength of the EMU, calculated and analyzed its stiffness and strength, and evaluated the results [15]. Rogulenko and others took the strength calculation of a general flat car body as an example to compare and analyze the calculation methods and evaluation standards in the strength specifications of railway freight car body in Russia and China [16]. Zaytsev and others improved the streamline of the car body on the E2 series 1000 high-speed train. By increasing the slenderness ratio of the head car, the micro air pressure wave when entering the tunnel was greatly reduced. They paid attention to the optimization of aerodynamic performance, and the car body was made of aluminum alloy [17]. Stopková and others take the TGV of the third-generation high-speed train as an example. On average, a trailer has only one bogie to carry. Under the condition of keeping the axle load no more than 17T, the total weight of each trailer is less than 34T [12]. Yuditskaya and others studied that an ice high-speed train body is welded with large extruded aluminum alloy profiles, without pillar and beam structure, so the self-weight is greatly reduced, and the axle load is less than 15t [18]. Based on the current research, this article puts forward the comparative analysis of railway flat car body strength calculation methods based on fuzzy logic and evolutionary algorithm. Based on fuzzy logic and evolutionary algorithm and taking the universal flat car body strength calculation as an example, this article makes an in-depth analysis of different body strength calculation methods in order to provide a more scientific and reliable theoretical basis for the structural strength design and analysis of railway flat car surveying and mapping. The experiment shows that in the strength design of the car body, the combination of longitudinal tensile load and vertical load should choose the combination of longitudinal compressive load and vertical maximum load. Because the synthetic stress is the largest under this combination condition, the safety of evaluating car body strength under this combination condition is higher. Compared with the traditional static strength allowable stress evaluation method, OREB12/RPL7 can qualitatively

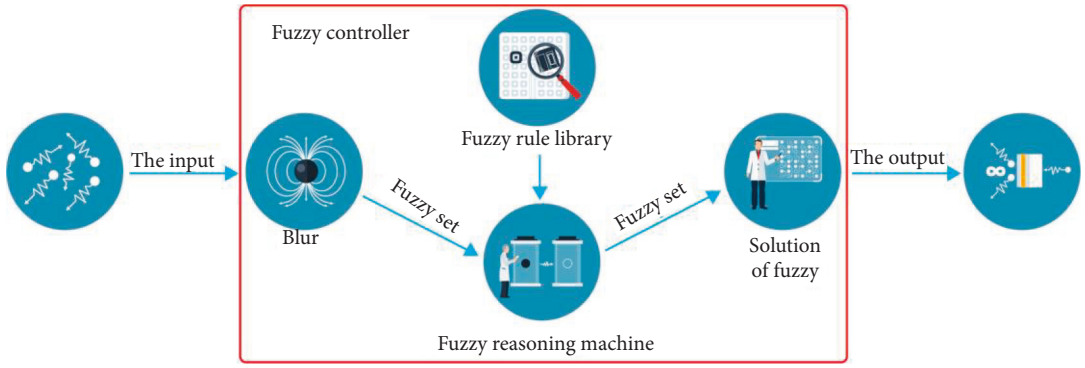

Figure 1: Fuzzy logic system.

analyze the fatigue strength allowance of the structure and evaluate the areas where the strength reserve of the car body is insufficient.

3. Fuzzy Logic System and Evolutionary Algorithm

3.1. Fuzzy Logic System

3.1.1. Concept. That is gray areas. For example, there is no obvious boundary between tall and short and fat and thin. It can be said that it is a little ot very high, so the boundary (or critical condition) is fuzzy [19]. To explain the above fuzzy ordering, we introduce the concept of membership: the value between 0 and 1 is the degree to which an event belongs to 0 or 1, that is, membership. We can write membership functions to judge membership or represent the probability of this state. Membership indicates rank. The higher its value, the higher the probability of this state. Instead, the probability of this state will be low. It is important to note that there are two basic principles of fuzzy logic systems. First, the meaning of fuzzy logic is to let computers take problems closer to human behavior. Second, the nature of fuzzy logic is about everything.

3.1.2. Basic Process. The uncertainty process consists of three main steps:

(i) Uncertainty: the process of obtaining membership from a certain set of uncertain inputs according to a membership function

(ii) Confirmation methods: methods for drawing fuzzy conclusions from ambiguous rules, membership in relevant fuzzy sets

(iii) Incompatibility: the process of turning ambiguous conclusions into clear and accurate outputs

The calculation process is roughly as follows:

Input (collection of specific data) ⟶ dimming (according to membership functions such as piecewise functions and distribution functions, and then get a set of fuzzy memberships (analytical data) from specific inputs).

Next, we will introduce each stage in the process of the fuzzy logic system in detail.

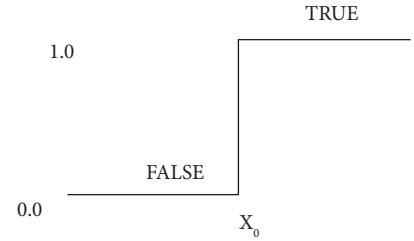

Figure 2: Boolean logic membership function.

In order to facilitate understanding, before discussing the membership function of fuzzy logic, we first talk about the membership function of traditional logic, such as Boolean logic. Figure 2 shows the membership function of Boolean logic [20].

There is no intermediate value between false and true, that is, nonblack or white, nonfalse or true in traditional logic. This is very unreasonable when making a judgment in real life. For example, if $x_0 = 170$ kg, anyone who exceeds 170 kg is overweight, and anyone who is less than 170 kg is not overweight. Even if someone is 169 kg, it is still regarded as not overweight. This is too extreme and impractical for judgment in daily life.

For the above traditional Boolean logic membership function, we can make a simple expansion and convert it into the membership function of fuzzy logic, as shown in Figure 3.

As can be seen from Figure 3, the gradual change is between 0 and 1. If it is less than x_0, the result will be false; that is, the membership degree is 0, while if it is greater than x_1, the result will be true; that is, the membership degree is 1. For values between x_0 and x_1, the membership varies linearly. We can easily give the membership equation:

$$f(x) = \begin{cases} \dfrac{x}{x_1 - x\_0} - \dfrac{x_0}{x_1 - x_0}, & x_0 < x < x_1. \\ 1, x \geq x_1 \end{cases} \quad (1)$$

If they weigh 185 kg, according to the calculation, their membership degree is 0.5; that is, they are a little overweight. Now there is a vague concept. In general, we consider how well the input variables correspond to indefinite sets in terms of membership functions. For example, we want to know if someone is overweight, underweight, or very healthy. For

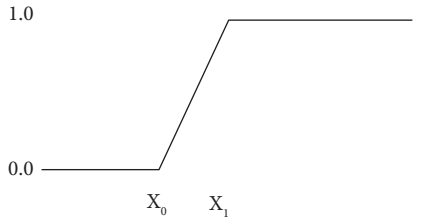

Figure 3: Membership function of simple fuzzy logic.

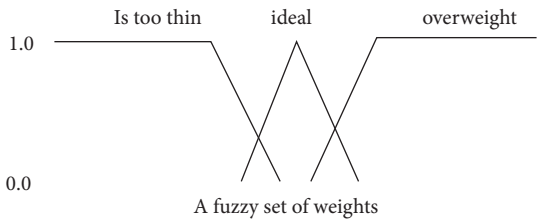

Figure 4: Fuzzy set of body weight.

this, we need to create a fuzzy set so that we can observe what interval the membership is in, depending on the membership function, which is its degree [21]. As shown in Figure 4, we assume a fuzzy set of three weights: too thin, ideal, and overweight.

With such a set, we can calculate the degree of membership for each input value in these three sets. If a person is thin, the membership is 0, the ideal membership is 0.75, and the overweight membership is 0.15. Then we can compare the membership degrees of the three fuzzy sets and come to the conclusion that the weight of this person is optimal, and the membership degree is 75% (0.75). Common membership functions include Gaussian membership functions, general bell membership functions, triangular membership functions, trapezoidal membership functions, and Z-shaped membership functions, as shown in Figures 5–7.

Like traditional logic operations, we introduce fuzzy logic operators intersection (AND), Union (OR), and complement (NOT) [22, 23].

After the fuzzy logic operation, we can get a multidimensional truth table and choose actions or scores according to the fuzzy results of each dimension. We take a simple example as an example of air combat [24]. According to the angle of our aircraft pointing to the opponent and the relative distance from the opponent, we give the score of "azimuth/distance situation." The higher the score, the more favorable the situation. Therefore, the fuzzy logic modeling is shown in Figure 8 and Table 1.

On the left are two fuzzy sets, namely, distance and pointing angle. On the right are fuzzy rules. The numbers in the table represent the azimuth/distance situation score. The higher the score, the more favorable the situation. For example, if the input data is blurred and the fuzzy results with close relative distance and positive pointing angle are obtained, we will check the table and get 3 points; that is, we think the situation is very favorable.

Fuzziness: when you want to use the exact value as the output data of the fuzzy system, you need to solve the fuzziness

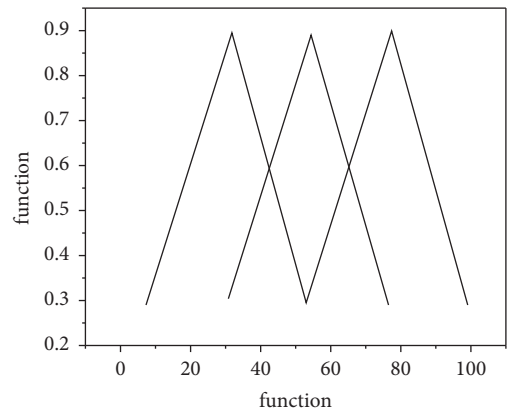

Figure 5: Triangular membership function.

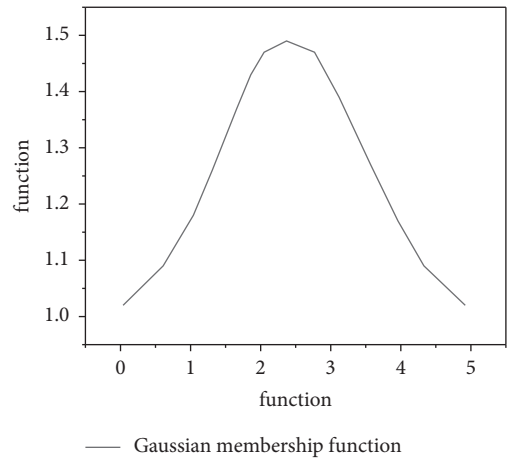

Figure 6: Gaussian membership function.

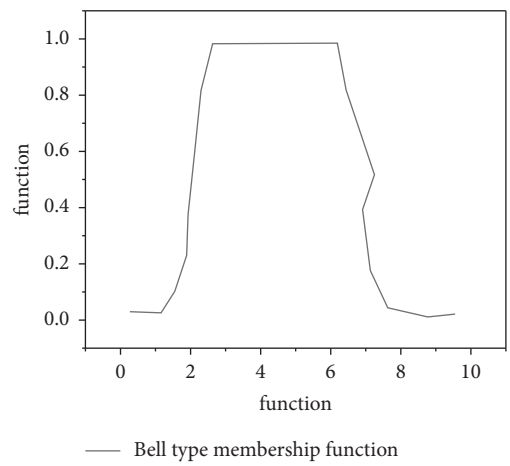

Figure 7: Bell membership function.

process [25]. As mentioned, each rule has some degree of membership in the outgoing set. The process of choosing a value that best represents an indeterminate set is called defuzzification. Commonly used methods include the

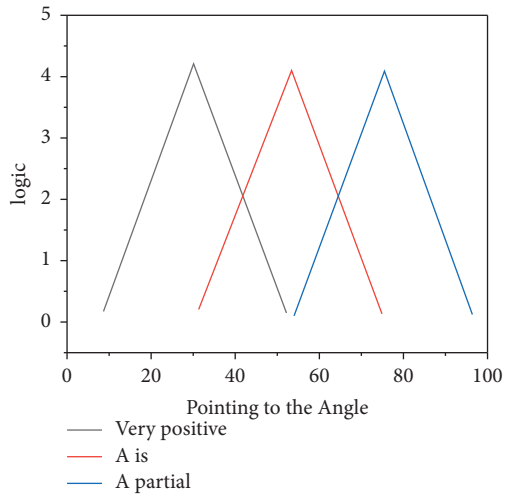

Figure 8: Fuzzy logic modeling of air combat example.

Table 1: Fuzzy rules.

Relative distance\pointing angle	Very positive	Relatively correct	More biased
Closer	3	2	1
Far away	2	2	1
Far	1	0	0

maximum membership method, the maximum average method, the field average method, and the center of gravity method.

3.1.3. Practical Application. In practical application, the fuzzy logic system involves the design of a fuzzy controller, including five main contents: fuzzy process (fuzzy method, fuzzy set division, and fuzzy function optimization), knowledge base (control rule type, consistency, completeness, and interaction), reasoning decision (fuzzy reasoning and defuzzification method), and optimization calculation (adjusting and optimizing fuzzy controller).

We use an example to illustrate how to design a fuzzy controller. An example is the inverted pendulum control system, as shown in Figure 9.

The controlled objects include an inverted simple pendulum, trolley, guide rail, and motor. Control scene: the single pendulum with a length of 2l and mass of M is fixed on the trolley with a mass of m by hinges. Through the hinge pendulum, the trolley can swing freely on a plane. The trolley is controlled by the motor and generates control force on the motor horizontally by means of electric current so as to make the trolley move on the limited guide rail and keep the inverted pendulum from falling down.

First, specify the input variables: angle ($-90^\circ \sim 90^\circ$) and angular velocity (real field); output variable: thrust (real field). Then we set the membership function to blur the input and output.

Five fuzzy sets of positive large, positive small, zero, negative small, and negative large are established, respectively, in the angle and angular velocity of input variables.

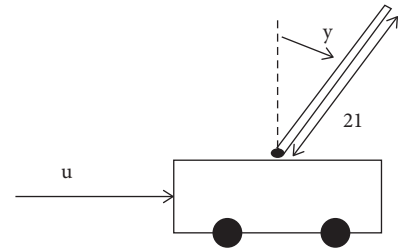

Figure 9: Inverted pendulum control system.

Table 2: Fuzzy rules.

Force u		"Change-in-error" $\dot{e}$ −2	−1	0	2	2
Error e	−2	2	2	2	1	0
	−1	2	2	1	0	−1
	0	2	1	0	−1	−2
	1	1	0	−1	−2	−2
	2	0	−1	−2	−2	−2

On the output variable thrust, five fuzzy sets are established: positive large, positive small, zero, negative small, and negative large. According to the fuzzy set, we establish fuzzy rules, as shown in Table 2.

Change-in-error refers to the angular velocity deviation, error refers to the angular deviation, and the values in the table refer to the fuzzy value of thrust u. For example, if we get that change-in-error is −2 and error is −2, we can find that u is 2 by looking up the table, which means that the current reverse deviation is very large, and we need a large forward thrust to balance the inverted pendulum. Then we use a defuzzification method to convert the output fuzzy value into a signal acceptable to the motor. For example, the center of gravity method is used to defuzzify. So far, the whole fuzzy controller has been designed.

3.2. Evolutionary Algorithm Calculation

3.2.1. Concept. Evolutionary algorithm borrows the law of biological evolution, realizes the survival of the fittest through reproduction, competition, reproduction, and recompetition, and approaches the optimal solution of complex engineering and technical problems step by step. Starting from the first set of randomly generated individuals in an evolutionary algorithm, the next generation of individuals is generated through three series of actions: duplication, exchange, and mutation, imitating the genetic mechanism of an organism. Then, according to the size of the fitness, do the best survival to improve the quality of the new generation group and gradually approach the optimal solution after repeated iterations. From a mathematical point of view, an evolutionary algorithm is basically a search and optimization method [26]. The main branches of evolutionary computing are as follows: genetic algorithm GA, genetic programming GP, evolutionary strategy ES, and evolutionary programming EP. Here we mainly introduce the genetic algorithm GA and evolution strategy ES.

3.2.2. Genetic Algorithm. The basic flow of the genetic algorithm is as follows.

Step 1. (gGroup startup). Plan the startup process according to the nature of the problem (the startup process should be as simple as possible, and the time complexity should not be too high), and start n groups. The second step: individual evaluation is used to calculate the physical fitness value of the individual group according to the optimal objective function.

Step 2. (repeat adjustment). Set the maximum number of iterations in the population to gmax, and the current number of iterations to be g = 1.

Step 3. (individual selection). The selected individuals enter the unified database to form the FP (g) of the first population to be traversed to form new individuals. The selection strategy should be based on the individual's physical abilities. If optimization is a mitigation problem, the odds of picking someone with a physical problem should be high. Common selection strategies include roulette selection and tournament selection.

Step 4. (crossover operator). The parent node will judge whether a crossover operation is required according to the crossover probability PM (prediction, generally 0.9). The crossover operator must be designed according to the properties of the optimal problem. This is the heart of all genetic algorithms. Its design will directly determine the performance of the entire algorithm.

Step 5. (mutation operator). according to the probability of PC mutation, the parents determine whether the individual needs to be mutated (predefined, generally 0.1). The main function of the mutation operator is to maintain the diversity of the population and prevent the local optimization of the population, so it usually takes the form of random transformation.

3.2.3. Comparison between Evolutionary Algorithm and Other Algorithms. Evolutionary computation and backpropagation algorithm: for supervised learning tasks that can directly and accurately calculate gradients, the evolutionary computation algorithm is not suitable in this scenario, but backpropagation is more efficient. Evolutionary computation becomes competitive in scenarios where the gradient of expected return needs to be estimated by sampling. In some scenarios, the backpropagation algorithm is difficult to adapt. For example, the reward is very sparse; that is, we have almost no labels for each sample, and there are rewards only in several specific states. In the scene where the reward is very sparse, the gradient is difficult to calculate. At this time, evolutionary computing has great advantages over backpropagation algorithms.

Reinforce-ES and TRPO: compared with TRPO, the performance of Reinforce-ES is similar, but the former has two characteristics.

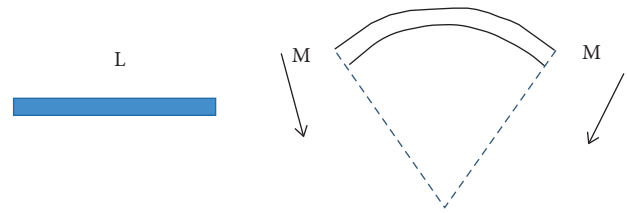

Figure 10: Schematic diagram of the definition of bending stiffness.

First, the data efficiency is poor. Reinforce-ES needs to constantly eliminate data, and most of the data is eliminated, so the data utilization is much worse than TRPO.

The second is very scalable. We take the difficult MuJoCo task as an example and use two algorithms for large-scale calculation. In the A3C algorithm, when assigning computing tasks to workers from the master node, all parameters of the network need to be assigned, and the computing cost is particularly high. The Reinforce-ES algorithm allocates only the fitness value of each iteration, only some scalars, so this algorithm is very efficient in large-scale computing engineering and is very suitable for this large-scale scenario.

4. Comparison of Strength Calculation Methods of Railway Flat Car Body

4.1. Strength Calculation of Vehicle Body. Take the length of a beam as L, the bending modulus of the section as I, and the elastic modulus of the material as E. Apply a unit relative bending angle θ at both ends of the beam, and the resulting end reaction moment M is the bending stiffness of the beam, as shown in Figure 10: the calculation formula is as follows:

$$K = \frac{M}{\theta}. \tag{2}$$

Simply supported beam with equal section:

$$\theta = \frac{ML}{EI}, \qquad K = \frac{EI}{L}. \tag{3}$$

Simply supported beam with variable section:

$$K = \frac{EI}{L}, \tag{4}$$

where I is the equivalent bending modulus.

Deflection and rotation angle are two basic quantities to measure bending deformation. This section will discuss the bending deformation of the simply supported beam under two loads. When the concentrated load acts on any point of the beam, the bending deformation deflection curve equation is as follows:

$$y = -\frac{Pbx}{6EIL}\left(L^2 - x^2 - b^2\right)(0 \le x \le a), \qquad y = -\frac{Pbx}{6EIL}\left[\frac{L}{b}(x-a)^3 + \left(L^2 - x^2\right)x - x^3\right](a \le x \le L). \tag{5}$$

Corner of end section:

$$\theta_A = \frac{Pab(L+b)}{6EIL},$$
$$\theta_B = \frac{Pab(L+a)}{6EIL}. \tag{6}$$

When $a > b$ is set, the following formula is satisfied:

$$x = \sqrt{\frac{L^2 - b^2}{3}}. \tag{7}$$

Based on the above formula, the following formula is satisfied:

$$y_{\max} = -\frac{Pb\left(L^2 - b^2\right)^{3/2}}{9\sqrt{3}EIL}. \tag{8}$$

The bending stiffness is as follows:

$$K = \frac{EI}{L} = -\frac{Pbx}{6yL_2}\left[\frac{L}{b}(x-a)^3 + \left(L^2 - x^2\right)x - x^3\right](a \le x \le L),$$
$$K = \frac{EI}{L} = -\frac{Pbx}{6yL^2}\left(L^2 - x^2 - b^2\right)(0 \le x \le a). \tag{9}$$

The bending stiffness expressed by the angle of the end section is as follows:

$$K = \frac{EI}{L},$$
$$\frac{EI}{L} = -\frac{\mathrm{Pab}}{6\theta_A L^2}(L+b), \tag{10}$$
$$-\frac{\mathrm{Pab}}{6\theta_A L^2}(L+b) = \frac{\mathrm{Pab}}{6\theta_B L^2}(L+a),$$

where P is the concentrated load force (unit: n); a and b are the distances between the front and rear support points and the load (unit: m); θ_A and θ_B are the rotation angles of the end section, that is, the rotation angle of the cross-section of the beam relative to its original position. It is specified that the counterclockwise rotation angle is positive (unit: RAD).

4.2. Comparative Analysis of Different Calculation Methods

4.2.1. Comparative Analysis of Vertical Maximum Operating Load. Typical domestic and foreign strength specifications mainly referred to in the strength calculation of high-speed train body in China include JISE7106, ENl2663 formulated by the European Railway Union, and the Interim Regulations on strength design test and appraisal of railway vehicles with a speed class of 200 km/h and above formulated by China (hereinafter referred to as the Interim Regulations). By comparing the above three specifications, the provisions on vertical running load are basically the same, except that the JISE7106 standard stipulates that the maximum vertical running load loaded on the vehicle body shall be considered according to the vibration during operation. If the secondary suspension device of the vehicle body adopts an air spring device, the maximum running load is $1.1 \times g \times (M1 + MZ)$. If the metal spring is used as the secondary suspension device of the vehicle body, the maximum operating load is $1.3 \times g \times (M1 + MZ)$ as specified in ENl2663. In the Interim Provisions, the maximum operating load is $1.2g \times (M1 + MZ)$. Through comparative analysis, it can be seen that JISE7106 fully considers the advantages that an air spring can better absorb vibration than a metal spring so as to reduce the vertical dynamic load caused by wheel–rail impact and vehicle spring vibration to $0.1g \times (M1 + MZ)$. It is stated in the Interim Provisions that the load in the application state may lead to material fatigue, so whether the maximum operating load is reduced to $1.2g \times (M1 + MZ)$ meets the design requirements and whether it can be considered separately according to the different secondary suspension devices like JISE7106 needs to be proved by test and actual measurement.

4.2.2. Comparative Analysis of Vehicle Load. There are two regulations on the jacking load in the European standard ENl2663: lift the vehicle at one end of the designated unwheeling space (2-point support), and its load is $1.1g \times (M1 + m3)$; lift the whole vehicle at the designated unwheeling position (4-point support), and its load is $1.1gm2 + m3$. The Japanese standard JISE7106 stipulates that the jacking load is 3-point support. There are two kinds of provisions on the jacking load in China's Interim Provisions: take the bogie at one end as the fulcrum and jack up the car body together with the bogie at the other end of the car body (2-point support), and the vertical load at this time is GX $(M1 + m3)$; when jacking up the whole vehicle body at the jacking positions at both ends of the vehicle body (4-point support), unbalanced factors (3-point support) shall be considered. At this time, the vertical load is $g \times m4$ (M3 bogie mass; M4 empty vehicle body mass).

Through comparative analysis, it can be seen that there are great differences in the provisions of jacking load in various specifications. In fact, when the vehicle is newly built and maintained, in the operation of jacking the vehicle body with jack, if the expansion and contraction of jack are not synchronous, the vehicle body will be in the state of three-point support. If the structure characterized by small torsional stiffness is adopted, the 3-point support state will produce permanent deformation. Therefore, the 2-point support, 3-point support, and 4-point support should be taken into account in the jacking load condition.

4.2.3. Comparative Analysis of Axial Load. By comparing the provisions on longitudinal load in European standard ENl2663, El, this standard JISE7106, and China's Interim Provisions, it can be seen that the three specifications not only have differences in the selection of longitudinal load conditions but also have different values. The provisions on longitudinal load in each standard are shown in Table 3.

Through the comparative analysis in Table 3, it can be seen that the Japanese standard JISE7106 takes a low value for the compressive load and tensile load at the coupler area,

Table 3: Comparison table of longitudinal load provisions in the standard unit: kN.

Working condition	Position	Standard		
		JISE7106	ENl2663	Interim provisions
Tensile load	Coupler	490	1000	1000
	Coupler	980	1500	1500
				1000
Compression load	End wall on the roof crosses the side wall on the upper side wall lower edge of the window. The end wall is above the floor above: 150 mm	Regulations need to be agreed with users	300	300
			300	300
			400	Nothing

and the specification directly uses the yield strength of the material as the allowable stress; that is, the safety factor is 1. Therefore, it is worth studying whether this standard can be used to evaluate the strength of the Chinese high-speed train body. The provisions of the Interim Provisions and ENl2663 on the compression and tensile load at the coupler are basically the same. However, the safety factor specified in the Interim Provisions is as high as 1.5, while the safety factor specified in EN12663 is only 1.15, which shows that the Interim Provisions have the highest requirements for the design of vehicle body strength and the corresponding design cost. However, considering that there is still a gap between China and foreign countries in terms of design, manufacturing, and process materials, the provisions in the Interim Provisions are relatively reasonable. The compression load in the end wall area mainly considers the strength and stability of the vehicle body under the condition of a train collision. JISE7106 has no clear provisions on the compression load in the end wall area but only needs to be negotiated with the user. The provisions of the Interim Provisions and ENl2663 on the longitudinal compressive load of the end wall area are basically the same, except that ENl2663 has an additional compression load condition of 400 kN acting on the end wall 150 mm from the floor.

4.2.4. Comparative Analysis of Torsional Load. Due to the irregularity of the line and the geometric error of vehicle manufacturing, the vehicle body in operation will produce torsional deformation. The provisions on torsional load in the Interim Provisions are that the torsional load of the vehicle body is taken as 40 kN *m*. The provision of torsional load in jlse7106 is that under the condition of ensuring that the spring device on one side does not rotate, the torsional load acting on the spring part on the other sides is 40 kN M. The torsional load is not specified in ENl2663, but it needs to be negotiated with the user. Through comparative analysis, it can be seen that the provisions on torsional load in JISE7106 are consistent with those in the Interim Provisions. The torsion of the car body has a great impact on the strength of the vehicle in operation, so the torsion load condition should be clearly specified in the car body strength specification.

4.2.5. Comparative Analysis of Combined Working Conditions. The European standard ENl2663 and the Japanese design general rule JISE7106 specify the combined working conditions as the longitudinal compression/tensile load and a maximum vertical load of the coupler, as well as the longitudinal compression/tensile load and vertical load of the coupler. The load superposition is shown in Tables 4 and 5. China's Interim Provisions are different from European standards and Japanese standards in the selection of combined working conditions. It is stipulated that the combined working conditions are the combination of longitudinal compression/tension load of the coupler and 1.3 times the maximum vertical load.

Table 4: Combined working conditions specified in EN12663.

Combined working condition	EN12663
Compression force and maximum vertical load	1 500 kN and $g \times (m^1 + m^2)$
Compression force and vertical load	1500 kN and $g \times m^1$
Tensile force and maximum vertical load	1 000 kN and $g \times (m^1 + m^2)$
Tensile force and vertical load	1000 kN and $g \times m^1$

Table 5: Combined working conditions specified in JIS E7106.

Combined working condition	JIS E7106
Compressive creep force and maximum vertical load	980 kN and $g \times (m^1 + m^2)$
Compression force and vertical load	980 kN and $g \times m^1$
Tensile force and maximum vertical load	490 kN and $g \times (m^1 + m^2)$
Tensile force and vertical load	490 kN and $g \times m^1$

According to the structural fatigue evaluation method given in the OREB12/RPL7 Research Report: the direction of fatigue crack and the direction of maximum principal stress are perpendicular to each other. Calculate the three-dimensional principal stress value and direction cosine of the node so as to determine the maximum and minimum principal stress values of the node under different load conditions, calculate the average stress and stress amplitude of the node according to the following formula, and finally evaluate the fatigue strength of the structure according to the modified Goodman fatigue limit diagram.

$$\sigma_m = \frac{\sigma_{\max} + \sigma_{\min}}{2},$$
$$\sigma_a = \frac{\sigma_{\max} - \sigma_{\min}}{2}. \quad (11)$$

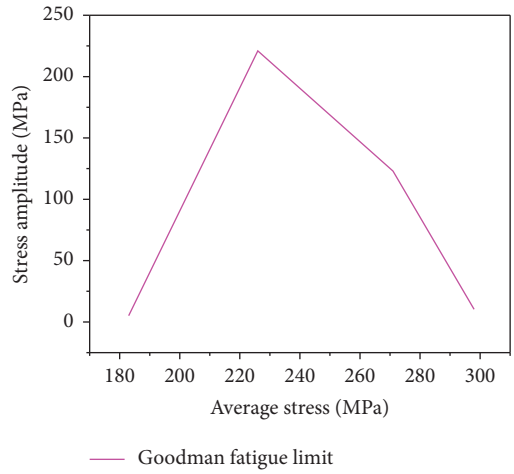

Figure 11: Goodman fatigue limit diagram.

4.3. Comparative Analysis of Fatigue Strength. ENI2663 stipulates that the load applied by the vehicle body during fatigue strength analysis is: vertical acceleration (1 ± 0.25) g and lateral acceleration (± 0.2) g. The evaluation of fatigue strength of the vehicle body in JISE7106 and Interim Provisions have not been clearly pointed out.

In this article, the fatigue strength of the car body is evaluated by two methods: according to the fatigue load conditions given in ENl2663, the magnitude and direction cosine of the three principal stress values at the stress concentration position are calculated, and then the fatigue strength of the car body is evaluated according to the ore fatigue evaluation method and the modified Goodman fatigue limit diagram. Select the parts with the maximum stress in the static strength analysis, calculate the size and direction of the three principal stress values of these parts, and then evaluate the fatigue strength of the car body according to the ore fatigue evaluation method (see Figure 11).

The results shown in Figure 11 show that from the fatigue strength analysis, the difference between the maximum principal stress and the corresponding allowable stress at the node where the maximum von Mises stress occurs is high, which is not the dangerous position of the structure. Under the specified service life, the stress of the selected key points is within the allowable range, and the car body structure meets the service requirements of fatigue strength. In the process of car body manufacturing, the welds in dangerous areas need to be processed to improve the fatigue strength of the weld area by reducing the stress concentration caused by welding.

5. Conclusion

This article presents a comparative analysis of the strength calculation methods of railway flat car body based on fuzzy logic and evolutionary algorithm. Through the comparison of the strength calculation methods of railway flat car body through the fuzzy logic system and evolutionary algorithm, it is concluded that three compression load conditions in the end wall area should be fully considered in the strength design of car body structure. In the strength design of the car body, the combination of longitudinal compression load and vertical load shall be selected as the combination of longitudinal compression load and vertical load because the synthetic stress under this combination condition is the largest, so the evaluation of the car body strength safety is more reliable. In the strength design of the car body, the combination of longitudinal tensile load and vertical load shall be the combination of longitudinal compressive load and vertical maximum load. Because the synthetic stress is the largest under this combination condition, the safety of evaluating car body strength under this combination condition is higher. Compared with the traditional static strength allowable stress evaluation method, OREB12/RPL7 can qualitatively analyze the fatigue strength allowance of the structure and evaluate the areas where the strength reserve of the car body is insufficient. In the future, the components of the high-speed test train body will be diversified, and the influence of the optimization results of its side wall on the optimization results of finishing remains to be investigated. It is expected to obtain comprehensive optimization results.

Data Availability

No data were used to support this study.

Conflicts of Interest

The author declares that there are no conflicts of interest regarding the publication of this article.

References

[1] D. Šipuš, T. Ležaić, J. Gašparík, and B. Abramović, "A comparative analysis of tariffs in regional railway passenger transport," *Transportation Research Procedia*, vol. 55, no. 2, pp. 196–203, 2021.

[2] V. A. Andreev, A. K. Bulkhin, B. V. Popov, and V. B. Popov, "Comparative analysis of shielding characteristics of signal-blocking cables for railway transport," *Radio Industry (Russia)*, vol. 30, no. 3, pp. 50–56, 2020.

[3] Z. Pater, "A comparative analysis of forming railway axles in 3- and 4-roll rolling mills," *Materials*, vol. 13, no. 14, p. 3084, 2020.

[4] A. V. Provorov, A. E. Lebedev, A. A. Vatagin, and D. A. Provorov, "Comparative analysis of methods for strength calculations of t-joints in process pipelines," *Chemical and Petroleum Engineering*, vol. 57, no. 5, pp. 370–375, 2021.

[5] T. Jiang, Y. Yu, X. Zhang, and W. Huang, "Comparative analysis of calculation methods for cable curve of landscape suspension bridges," *Journal of Physics: Conference Series*, vol. 1624, no. 4, Article ID 042043, 2020.

[6] E. Sudoł, E. Szewczak, and M. Malek, "Comparative analysis of slip resistance test methods for granite floors," *Materials*, vol. 14, no. 5, p. 1108, 2021.

[7] H. Chen, D. Fan, J. Huang, W. Huang, G. Zhang, and L. Huang, "Finite element analysis model on ultrasonic phased array technique for material defect time of flight diffraction detection," *Science of Advanced Materials*, vol. 12, no. 5, pp. 665–675, 2020.

[8] F. I. Ovi and R. J. Shova, "Comparative analysis of technical parameters of different knitted structures (Jersey, pique and lacoste) with or without lycra/spandex," *Journal of Textile Science and Technology*, vol. 08, no. 01, pp. 68–87, 2022.

[9] L. F. de Assis, C. C. Lemes Filho, G. Teixeira de Paula, and B. Pinheiro de Alvarenga, "Comparative analysis of different methods associated to the frozen permeability method for on-load cogging torque evaluation in permanent magnet synchronous machines," *IEEE Latin America Transactions*, vol. 19, no. 02, pp. 199–207, 2021.

[10] K. Sakouvogui and M. Bahmanioskoo Ee, "A comparative approach of stochastic Frontier analysis and data envelopment analysis estimators: evidence from banking system," *Journal of Economics Studies*, vol. 47, no. 7, pp. 1787–1810, 2020.

[11] S. Chawla, J. T. Shahu, and S. Kumar, "Analysis of cyclic deformation and post-cyclic strength of reinforced railway tracks on soft subgrade," *Transportation Geotechnics*, vol. 28, no. 8, Article ID 100535, 2021.

[12] V. Zitrický, V. Ľupták, O. Stopka, and M. Stopková, "Comparative analysis in terms of environmental impact assessment between railway and air passenger transport operation: a case study," *International Journal of Sustainable Aviation*, vol. 6, no. 1, p. 21, 2020.

[13] K. Hoterova, "Comparative analysis of the resilience and vulnerability of the railway infrastructure," *MEST Journal*, vol. 8, no. 2, pp. 100–106, 2020.

[14] P. Xu, Z. Sun, S. Shao, and L. Fang, "Comparative analysis of common strength criteria of soil materials," *Materials*, vol. 14, no. 15, p. 4302, 2021.

[15] W. Hongyan and W. Wen, "Comparative analysis of civil engineering quantity calculation based on glodon gtj and revit," *IOP Conference Series: Earth and Environmental Science*, vol. 791, no. 1, Article ID 012052, 2021.

[16] T. M. Rogulenko and A. A. Bondarenko, "Planning and analysis methods of revenues and expenses by individual activities of railway transport companies," *Upravlenie*, vol. 8, no. 1, pp. 63–72, 2020.

[17] V. A. Zaytsev, M. O. Pleshkov, D. N. Starkov, V. P. Demkin, T. V. Rudenko, and H. Kingma, "Comparative analysis of oculography methods for the diagnosis of the vestibular system," *Russian Physics Journal*, vol. 64, no. 10, pp. 1845–1849, 2022.

[18] A. S. Yuditskaya and S. S. Tkachev, "Comparative analysis of methods for modeling the gravitational potential of complex shaped bodies," *Mathematical Models and Computer Simulations*, vol. 13, no. 6, pp. 1138–1147, 2021.

[19] A. Santana, A. Pedrotti, F. Oliveira et al., "Comparative analysis of sustainability assessment methods in agro-ecosystems," *International Journal for Innovation Education and Research*, vol. 9, no. 4, pp. 164–182, 2021.

[20] N. Bhatt, S. Soni, and A. Singla, "Comparative analysis of numerical methods for constitutive modeling of shape memory alloys," *Modelling and Simulation in Materials Science and Engineering*, vol. 29, no. 8, Article ID 085012, 2021.

[21] R. G. Bolbakov, A. V. Sinitsyn, and V. Y. Tsvetkov, "Methods of comparative analysis," *Journal of Physics: Conference Series*, vol. 1679, no. 5, Article ID 052047, 2020.

[22] K. F. Hasan, O. K. Fayadh, and Q. F. Hasan, "Design engineering design and analysis of flat and grid slab system with conventional slab comparative approach," *Design Engineering*, vol. 2021, no. 7, pp. 1628–1649, 2021.

[23] M. Murillo, D. Abudinen, M. D. Río, N. Serrato, L. Patrón, and J. Ramírez, "Comparative analysis of the compressive strength of concrete under different curing methods," *IOP Conference Series: Materials Science and Engineering*, vol. 1126, no. 1, Article ID 012002, 2021.

[24] V. Marchuk, I. Shrayfel, G. Hripkov, and I. Nikishin, "Comparative analysis of methods for calculating the mode of a stationary random process," *E3S Web of Conferences*, vol. 279, no. 3, Article ID 02004, 2021.

[25] C. Sanitha Michail, "Comparative analysis of solution methods for swing equation in power system for transient stability studies," *IOP Conference Series: Materials Science and Engineering*, vol. 1166, no. 1, Article ID 012053, 2021.

[26] A. Ramesh Khaparde, F. Alassery, A. Kumar et al., "Differential evolution algorithm with hierarchical fair competition model," *Intelligent Automation & Soft Computing*, vol. 33, no. 2, pp. 1045–1062, 2022.